Materiales de Construcción
Vol. 72, Issue 346, April-June 2022, e284
ISSN-L: 0465-2746
https://doi.org/10.3989/mc.2022.17321

Characterization of DEF affected concretes: detection and modification of properties

A. Pichelin[a,b], M. Carcassès[a], F. Cassagnabère[a]✉, S. Multon[a], G. Nahas[b]

Laboratoire Matériaux et Durabilité des Constructions (LMDC), Toulouse University 3 INSA, (Toulouse, France)
Institute for Radioprotection and Nuclear Safety (IRSN), (Fontenay-aux-Roses, France)
✉: franck.cassagnabere@insa-toulouse.fr

Received 21 November 2021
Accepted 4 April 2022
Available on line 1 June 2022

ABSTRACT: The evolutions of the different physicochemical and mechanical properties as a function of the expansion due to Delayed Ettringite Formation (DEF) in concrete are studied. In comparison of sound materials, some characterizations were made in accordance to the level of expansion: in the initial time, in the latent period, in the accelerating phase and at the end of expansion. The characterization was as follows; SEM analysis was used to observe the presence of DEF. Physical tests linked to transfer properties; gas permeability and electrical resistivity were measured to detect micro-cracks generated by the DEF advancement. To observe the impact of micro-cracks, compressive strength and static modulus were experimentally determined. It was observed that few tests can be used to detect theses pathologies earlier, during the latent period. Gas permeability, electrical resistivity and elastic modulus results were promising. These tests are very sensitive to the development of micro-cracks generated in the concrete by the development of swelling due to DEF.

KEY WORDS: Delayed ettringite formation (DEF); Durability indicators; Detection; Monitoring; Swelling.

Citation/Citar como: Pichelin, A.; Carcassès, M.; Cassagnabère, F.; Multon, S.; Nahas, G. (2022) Characterization of DEF affected concretes: detection and modification of properties. Mater. Construcc. 72 [346], e284. https://doi.org/10.3989/mc.2022.17321.

RESUMEN: *Caracterización de hormigones afectados por DEF: detección y modificación de propiedades.* Se estudia la evolución de las diferentes propiedades fisicoquímicas y mecánicas en función de la expansión debida a la formación de etringita diferida (DEF) en el hormigón. En comparación con los materiales de referencia, se realizaron caracterizaciones de acuerdo al nivel de expansión: en el tiempo inicial, en el período latente, en la fase de aceleración y al final de la expansión. La caracterización fue la siguiente: se utilizó análisis SEM para observar la presencia de DEF, se realizaron pruebas físicas vinculadas a las propiedades de transferencia, y se midieron la permeabilidad al gas y la resistividad eléctrica para detectar micro-fisuras generadas por el avance de DEF. Para observar el impacto de las micro-fisuras, se determinaron experimentalmente la resistencia a la compresión y el módulo estático. Se observó que pocas pruebas pueden utilizarse para detectar estas patologías antes y durante el período de latencia. Los resultados de la permeabilidad al gas, la resistividad eléctrica y el módulo elástico fueron prometedores. Estos ensayos son muy sensibles al desarrollo de micro-fisuras generadas en el hormigón por el desarrollo de hinchamiento debido a la DEF.

PALABRAS CLAVE: Formación de etringita diferida (DEF); Indicadores de durabilidad; Detección; Supervisión; Entumecimiento.

This article was selected among the papers presented at the 2022 *International Conference on Alkali-Aggregate Reaction in Concrete* (16th ICAAR)

1. INTRODUCTION

Many engineering structures (dam, bridge, nuclear structure) are susceptible to develop Internal Sulfate Attack (ISA) by Delayed Ettringite Formation (DEF). This reaction requires the presence of three main factors: high sulfate and aluminate contents, water, and a rise in temperature of concrete. This reaction leads a swelling of concrete materials generating microcrack, cracks, loss of material performances and structure damage.

The reaction mechanisms of DEF are complex. Brunetaud (1) has proposed a global mechanism, described in four phases, grouping many theories to explain swelling (crystallisation pressure (2), osmotic pressure (3), homogeneous swelling (4), swelling at the Interfacial Transition Zone (5), electric double layer (6). The swelling can be represented by a sigmoidal curve of expansion of the time in various regime (1). This first phase corresponds to the dissolution of the primary ettringite. Secondly and under certain conditions, the latent period can begin (low expansion) with the precipitation of delayed Ettringite in the microstructure (porosity, Interface Transition Zone (ITZ), Hadley grain). When the tensile strength of concrete is reached due to internal pressure, cracks were generated (end of latent period). Thirdly, after an inflection point, the precipitation of delayed Ettringite in cracks, leads to cracks propagation. It is the acceleration of expansion. Finally, the deceleration of swelling occurs when one reactant is consumed and/or when the cracks opening is sufficiently significant to accommodate new products without generation of supplementary expansion.

Several parameters have an influence on the development of DEF, and can be divided into two groups: those related to the formulation of concrete (binder nature (7), Water / Cement ratio (8) and those related to the environment (temperature curing (9, 10), relative humidity (11, 12)).

Main consequences of DEF are expansion and cracks. They affect the physicochemical and mechanical properties of the concrete. Cracks lead to an increase of transfer properties and a decrease of mechanical properties (12) and may lead to a loss of tightness, which is harmful for nuclear power plants. Few data can be found in the literature on the evolution of these properties as a function of the degree of advancement of DEF. The present study had two objectives: first, to find a sensitive test allowing DEF to be detected before cracking can be observed visually and, second, to evaluate the evolution of the properties that impact the tightness and also the durability of concrete. A test protocol to accelerate DEF development was carried out and provided a good representation of the reality on site (13). A large number of samples were used to characterize the impact of DEF on concrete properties at different levels of expansion. Chemical tests were performed to observe the initiation and the presence of DEF, while physical and mechanical tests evaluated the impact of DEF on mechanical and transfer properties.

2. EXPERIMENTAL PROGRAM

2.1. Concrete

2.1.1. Cement and aggregates

In this study, two cements and two types of aggregates were used. The choice of cements focused on a CEMI 52.5N and a CEMII/A-LL 42.5 (14), the main characteristics of which are summarized in Table 1.

Siliceous and limestone aggregates were used as described in the Mix designs subsection. These two cements have been used in previous studies and show a high swelling potential in the case of DEF, in particular because of their high sulfate, alkali and aluminate contents (12, 13).

Table 1. Cement compositions.

Mass content (%)	CEM I 52.5 N	CEMII/A-LL 42.5 R
SiO_2	19.3	19.7
CaO	63.2	63.5
Al_2O_3	5.3	4.6
Fe_2O_3	2.6	3.2
K_2O	0.94	1.36
Na_2O	0.08	0.11
SO_3	3.5	2.7
Total	94.92	95.17

2.1.2. Mix designs

The mix designs have already been studied in other experimental works, which make it possible to complete the database on the behavior of these concretes (12, 13). However, some modifications were made in the nature of aggregates used. Indeed, the limestone aggregates used in (12, 13) contain a part of siliceous phase which is not qualified with respect to the risk of Alkali-Silica Reaction (ASR).

The proportion of aggregates was determined with respect to Dreux method in order to reproduce the same aggregate skeleton. A lot of tests are performed in this study; the use of data from previous studies (12, 13) is therefore not useful. The formulations are detailed in Table 2. The sampling is done in (11 x 22) cm^3 cylindrical molds (Figure 1).

The choice of siliceous and limestone aggregates respectively with CEMII and CEMI was conducted to reproduce mix design representative of nuclear structures. They have also been used for concrete blocks, as part of a new platform (ODOBA project (15)) test developed by the Radioprotection and Nuclear Safety Institute (IRSN), to study the impact of DEF degradation at scale structure. The concrete casting procedure used in this study followed the protocol of French standards (16, 17).

TABLE 2. Mix designs of "CEM II-Si" (a) and "CEM I-Ca" (b) concrete.

(a) CEM II-Si		(b) CEM I-Ca	
Material	**Content (kg/m³)**	**Material**	**Content (kg/m³)**
CEM II/A-LL 42.5 R	350		
0/0.315	264	CEM I 52.5 N	400
0.315/1	151	0/4	718
1/4	254	4/11.2	289
4/8	145	11.2/22.5	813
8/12	399	Effective water	185
12/20	616		
Effective water	188		

2.2. Conditioning

French-recommended performance test for DEF-reactivity MLPC #66 was adopted (18) in order to allow a rapid development of DEF. This test comprises four stages: concrete mixing, heat treatment, dry/wet cycles, and final immersion of samples in water at 20°C. The thermal treatment at early age corresponded to that in Al Shamaa's study (12).

Once cast, specimens were placed in a climate chamber at controlled temperature and relative humidity. In container (Figure 2), the heat treatment was applied for 7 days and comprised four stages: a hold at 20°C, 95% RH for 2h, followed by a rise in temperature from 20°C to 80°C, 95% RH at a rate of 2.5°C/h, stabilization at 80°C, 95% RH for 72h and a temperature decrease from 80°C to 20°C, 95% RH at a rate of 1°C/h (Figure 3a). The effective thermal energy (10) generated by the heat treatment was 1395°C.h.

The selected dry/wet cycles correspond to the French-recommended performance test for DEF-reactivity MLPC #66 (18). They are composed of two 14-day cycles: drying at 38°C, HR < 30% for 7 days and humidification in water at 20°C for 7 days (Figure 3a). These cycles allow the initiation of micro-cracking in the concrete and thus accelerate the kinetics of DEF appearance within the concrete without increasing the amplitude of the deformations (19). The beginning of the degradation is considered to occur at 35 days, at the end of the heat treatment and dry/wet cycles, in this case. During the first 35 days, the concrete is considered to be in a state of hydration where no expansion due to DEF develops. The storage water was not renewed.

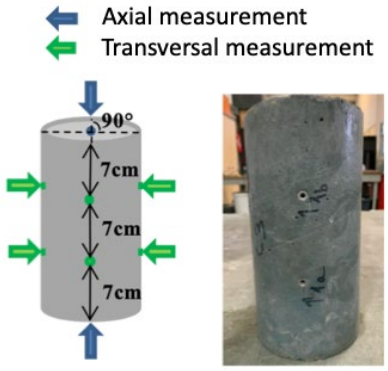

FIGURE 1. Cylindrical specimen for expansion measurement.

When the dry/wet cycles had been completed, the samples were stored in isothermal containers at 20°C (Figure 2), equipped with a pump to homogenize the temperature and the species present in the water.

The reference specimens underwent the same elaboration process but were not subjected to the heat treatment. During the first 7 days, the reference specimens were stored in water at 20°C. Dry/wet cycles were also applied (Figure 3b).

2.3. Testing protocols

The mass and expansion monitoring were performed on three cylindrical test pieces 11 x 22 cm³ (Figures 1, 4 and 5.a). Studs were fixed directly on the mold and were therefore embedded in the concrete. Longitudinal expansion was measured by a digital micrometer having an accuracy of ±1 µm.

FIGURE 2. Conservation containers for DEF development.

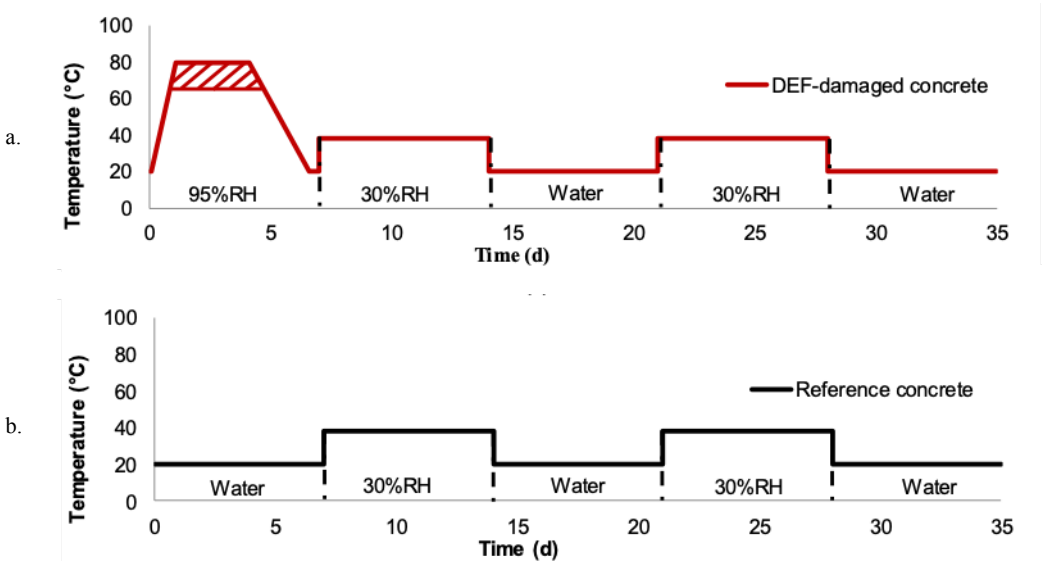

FIGURE 3. Thermal profile of concretes developing DEF and dry/wet cycles for both concretes (a. for concretes developing DEF - b. for reference concretes).

The transversal expansion was measured by a micrometer having an accuracy of ±5 µm.

Microscopic observations were performed to ensure the presence of DEF in the concrete (Figure 5.b). SEM observation in BSE mode and chemical analysis with EDS were realized. When the swelling was initiated (expansion of 0.04%), measurement of the physical properties (Figure 4) revealed the impact of the micro-cracking generated on the transfer properties. Finally, measuring the mechanical properties gave some indications on the level of damage of the concrete subjected to these pathologies. Measurements of all the properties were made at different levels of expansion.

2.3.1. Physical characteristics

Two physical tests were performed: electrical resistivity and gas permeability. The electrical resistivity test (Figure 5c) was performed on three (11 x 5) cm^3 cylindrical samples obtained from an (11 x 22) cm^3 one, in accordance to the Perfdub protocol (20). This test was performed to complete the concrete database of this new test protocol. The gas permeability test (Figure 5d) was performed according to the standards (21) but the drying temperature was adapted to this study and did not correspond to that proposed in the standard (105°C). It was set at 40°C to avoid destabilizing the delayed Ettringite formed in hardened concrete. The damage generated during drying is also reduced. Samples are dried until mass stabilization (0.05% after 7 days).

2.3.2. Mechanical characteristics

Two mechanical properties were measured: the compressive strength (Figure 5e) and the elastic modulus (Figure 5f). These properties were measured on three (11 x 22) cm^3 cylindrical specimens according to the standards (22, 23).

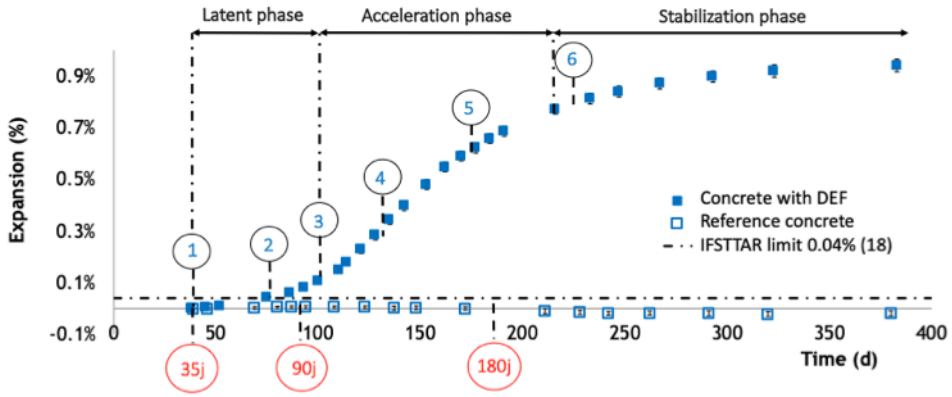

FIGURE 4. Summary of measurements: for DEF concrete, in blue (1 to 6) depending of expansion; for reference concrete, in red depending of time (35, 90 and ≈180 d).

Table 3 summarizes the test performed in this study (number and size of specimens, reference and repeatability). Figure 5 shows all the tests performed on concrete materials.

3. RESULTS

3.1. Expansion

Figure 6 shows the evolution of expansion as a function of time for the two concretes and their corresponding reference concrete. French-recommended performance test for DEF-reactivity MLPC #66 refers to a swelling limit of 0.04% in an expansion test (18). This limit is provided up to 12 months test duration. Beyond this threshold, there is a risk of the concrete to be damaged by DEF. The reference formulations did not exceed the limit threshold and showed a maximum swelling of 0.02%. The expansion curve due to DEF can usually been described as a sigmoid (Figure 6), with three phases:

- The latent period is characterized by the precipitation of DEF in the microstructure (porosity, Interface Transition Zone (ITZ), Hadley grain) (1). Expansion is small in this period. When the tensile strength of concrete is reached due to internal pressure, cracks were generated. The end of latent period is marked by the inflection point.
- The precipitation of DEF in cracks, leads to cracks propagation and so to the acceleration of expansion.
- Finally, the deceleration of swelling occurs when one reactant is consumed and/or when the cracks opening is sufficiently significant to accommodate new products without generation of supplementary expansion (1).

Specimens developing DEF showed significant swelling, around 0.9%, at the end of the expansion

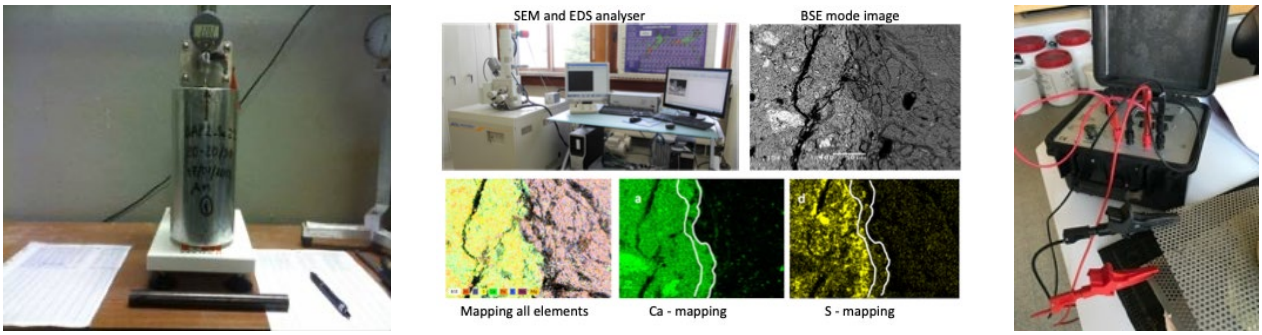

a. Expansion and mass monitoring

b. Microscopic analysis (SEM + EDS)

c. Electrical resistivity

d. Gas permeability

f. Elasticity modulus

e. Compressive strength

FIGURE 5. Experimental tests set-up.

TABLE 3. Summary of performed tests, number and size of samples used.

	Number / size of samples	Test references	Test repeatability (%)
Mass and expansion	3 (∅11 x 22) cm^3		-
Microscopic observations	/		-
Electrical resistivity	3 (∅11 x 5) cm^3	Perfdub, 2017	10.5
Gas permeability	3 (∅11 x 5) cm^3	XP P18-463	11.1
Compressive strength	3 (∅11 x 22) cm^3	NF EN 12390-3	8.0
Modulus of elasticity	3 (∅11 x 22) cm^3	NF EN 12390-13	-

for CEMII-Si. The end of the latent period, marked by the inflexion point, was at 80 days for the CEMI-Ca and 110 days for the CEMII-Si concrete. In comparison with the CEMII-Si concrete, CEMI-Ca contained large limestone aggregates that lead to a decrease of the latent period (14). This phenomenon is attributed to the higher bonding in case of limestone aggregates with the cement matrix. In this case, cracks generated at the Interfacial Transition Zone (ITZ) during the heat treatment due to a differential dilatation coefficient between paste and aggregates, were reduced (24). On one hand, the low cracking results in a lower volume available to accommodate the new phases due to DEF without inducing cracking and expansion. On the other hand, the low cracking leads to a decrease of transfers properties in concrete and thus to delay DEF expansion. The both phenomena are opposed. Indeed, a decrease in transfer properties cannot explain the lowest latent period observed in the case of limestone aggregates. The decrease in available volume caused by the low cracking at the ITZ therefore seems to be the cause of the decrease in latent period. In this case, the volume of DEF necessary to generate pressure is reduced and it leads to a decrease of latent period.

The final expansion of CEMI-Ca showed a swelling of around 0.6%. This lower swelling was attributed to the presence of limestone aggregates, which allowed the bond between aggregate and cement paste to be increased by the formation of calcium hydrates around the aggregates (25-27). The cracks generated by DEF at the ITZ were also reduced, allowing a lower final expansion (25, 27). Moreover, the difference between concretes composition with a higher Water / Cement ratio (W/C) and a higher amount of cement could also explain the higher swelling observed.

The longitudinal and transversal expansion measurements are very close, and lead to fairly isotropic expansions. These results are in accordance to the isotropy of the swelling already observed in stress free conditions (28, 29). However, the transversal swelling is slightly lower on the CEMII-Si concrete at the end of expansion.

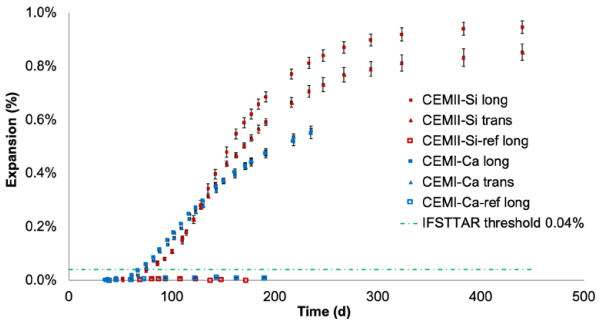

FIGURE 6. Evolution of expansion (transversal and longitudinal) versus time.

3.2. Microscopic observations

The presence of delayed Ettringite was observed by SEM for each level of expansion.

Figure 7 shows the presence of delayed Ettringite in massive and compressed form for different levels of swelling (in red circle on the SEM images – BSE mode), in the CEMII-Si concrete where siliceous aggregates were used. The SEM images show that the initiation of swelling was induced by the formation of delayed ettringite in Hadley grains (Figure 7a) and at the ITZ (Figure 7b) (expansion of 0.05%). As expansion continued, delayed Ettringite continued to develop in these areas and in the porosity (Fig-

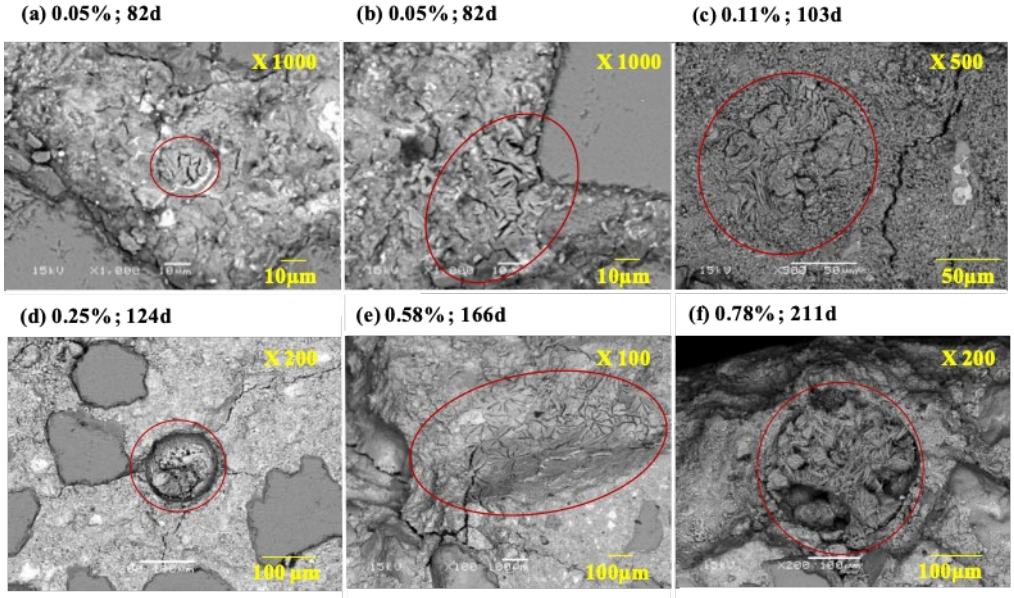

FIGURE 7. SEM images of the CEMII-Si concrete.

ure 7c and 7d). Then there was a separation from the cement paste all around the aggregates (Figure 7d). At the time corresponding to 0.25% of swelling, the cracks propagated from the ITZ to the porosity, causing an acceleration of swelling. When expansion continued, the presence of delayed Ettringite became increasingly significant, both in the cement paste (Figure 7e) and in the porosity (Figure 7f).

The SEM observations on the CEMI-Ca were consistent with those observed on the CEMII-Si concrete. However, cracking generated at the ITZ in the case of limestone aggregates did not propagate all around the aggregate particles, thus confirming the observations of Yang et al. (27).

For each design, the presence of delayed Ettringite is found first at the ITZ, in the Hadley grains and in the porosity. Ettringite then propagates in and between these preferential zones, generating more and more cracking. This cracking marks the acceleration of the expansion. As mentioned above, the cracking generated at the ITZ depends on the nature of the aggregates (27). In the case of siliceous aggregates, cracking is generated all around the aggregate but it only partially surrounds when limestone aggregates are used. Ettringite then spreads in existing cracks. From SEM image in Figure 8a (Back-Scattered Electrons mode - BSE mode in Figure 8a), Figure 8b shows the presence of sulfur in the sample (yellow trace in Figure 8b), proving the presence of delayed ettringite in concrete cracks. These observations confirm that the cracks caused by the DEF are filled with ettringite during the expansion. These results agree with the theory of swelling proposed by Brunetaud (1).

3.3. DEF Detection

One of the first aims of this experimental program was to find a sensitive test allowing DEF detection. DEF can be detected if the evolution of one of the properties measured in this work is significant (sufficiently higher than the scatter on results) and only due to DEF expansion (not to concrete hydration). In this aim, a DEF detection criterion for physical and mechanical properties was developed, taking the effect of hydration (ageing) and experimental scatter into account (Equation [1]):

$$X_{i\,threshold}(t) = X_0\left(1 + \frac{X_{i\,ref}(t) - X_{0\,ref}}{X_{0\,ref}}\right) \pm 2\overline{\sigma_{ref}} \quad [1]$$

With: $X_{i\,threshold}(t)$ the threshold value of detection of the property measured in time,
X_0 the initial value of the pathological concrete,
$X_{0\,ref}$ the initial value of the reference concrete,
$X_{i\,ref}(t)$ the value of the property of the reference concrete in time, $\overline{\sigma_{ref}}$ the average of the standard deviations obtained on the reference specimens.

These threshold values are used for the detection of DEF, presented in the charts for each pathological concrete (Figures 9 and 10). The evolution part of properties due to hydration was considered by the measurement of reference concretes at 35, 90 and 180 days (Figure 4). This evolution might be different between pathological and reference concrete due to the thermal treatment in case of pathological concretes. However, it provides an estimation of the evolution of the properties if no pathology was developed. The evolution of threshold values is considered as constant between two property measurements (35, 90 and 180 days).

3.4. Physical properties

These tests were performed on three concrete samples. The average of the three measurements is represented on the charts. The associated standard deviations are also represented. The resistivity values and apparent permeability coefficients are given on time for the reference concretes (CEMII-Si and CEMI-Ca) in Table 4.

The electric resistivity tests (Figure 9a) showed a great sensitivity. Reference concretes CEMII-Si-ref and CEMI-Ca-ref had a resistivity of 45 Ω.m at 35 days. The concretes developing the pathology had a lower resistivity, around 35 Ω.m, at the same

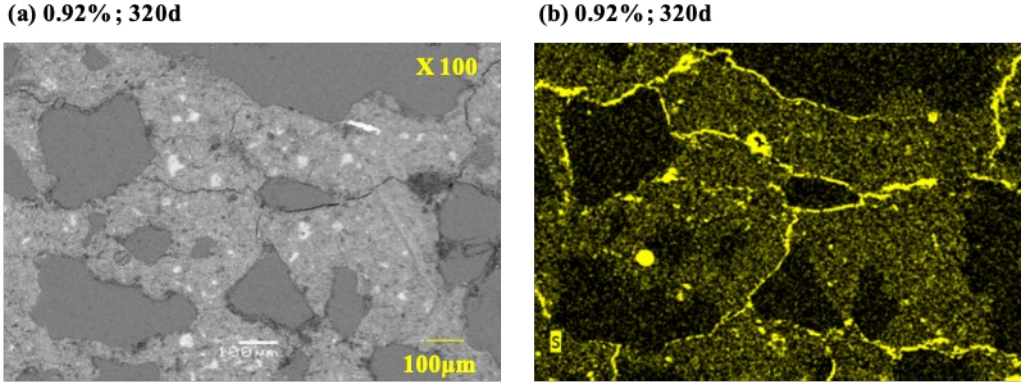

FIGURE 8. CEMII-Si SEM images (a) BSE image and (b) sulfur image (mapping).

time, the heat treatment having caused additional damage. These values lead to a variation of about 4.2 Ω.m (test repeatability of 10.5%).

In Figure 8a, a progressive decrease in the resistivity is observed during the damage. A stabilization around 25 Ω.m is reached at 0.3% of expansion. This stagnancy could be due to the cracking caused by the pathology being gradually filled by ettringite. In contrast, for the reference concretes, the electrical resistivity increased significantly between 35 and 90 days. A resistivity increases of 25% was observed from day 35 to day 180, due to the evolution of the hydration reactions, illustrated by the increase in threshold values during the expansion.

With the chosen criterion, the detection of DEF by the electrical resistivity took place between 0.05 and 0.1% of expansion, during the latent period. Between these two expansion levels, the decrease of resistivity was sufficient to point out significant damage.

Figure 9b shows the evolution of the apparent air permeability coefficient as a function of the expansion generated by DEF. First, the reference concretes CEMII-Si-ref and CEMI-Ca-ref show no change in their coefficients of permeability on time of 110×10^{-18} m² (Table 4).

The CEMII-Si and CEMI-Ca concretes have similar apparent gas permeability, respectively equal to 125×10^{-18} m² and 60×10^{-18} m² before expansion. These values lead to a variation of 14×10^{-18} m² and 6.6×10^{-18} m² (test repeatability of 11.1%) respectively for CEMII-Si and CEMI-Ca concretes. During expansion, the CEMII-Si concrete shows a strong increase in the coefficient of permeability at the beginning of expansion (permeability at 0.05% is double that before expansion). The CEMI-Ca also shows an increase but it occurs later and is smaller. This difference could be due to a higher damage of CEMII-Si concrete during the thermal treatment (see 3.5) but also due to the mineralogical nature of the aggregates used. The ITZ of concretes containing limestone aggregates seem to be improved (25-27). Cracks due to DEF passing through this interface are reduced in the case of limestone aggregates (27). There may be fewer preferential paths in the CEMI-Ca concrete, causing a smaller increase of permeability at early expansion. When the acceleration phase of the pathology is reached, at around 0.2% of swelling, the permeability is significantly impacted. This drastic increase can be attributed to the formation of more and more percolating paths within the material, generating a large increase of gas flow during the test. These results are therefore in agreement with those of Al Shamaa et al. (12).

Depending on the chosen criterion, the detection of DEF by the measurement of gas permeability takes place during the latent period before 0.05% expansion for CEMII-Si concrete and at the beginning of the acceleration phase, between 0.17 and 0.29%, for CEMI-Ca concrete. However, the range of expansion at the detection for CEMI-Ca concrete is excessive regarding the appearance of visual defects of about 0.12% of expansion (12, 30).

TABLE 4. Physical values for reference concretes on time (average values and deviation standard).

CEMII-Si-ref	35 d	91 d	180 d
Elec. resist. (Ω.m)	45.0 (2.2)	55.0 (3.8)	58.0 (4.9)
Appar. permea. (10^{-18} m²)	108.2 (16.8)	103.6 (9.8)	101.2 (27.3)
CEMI-Ca-ref	35 d	90 d	180 d
Elec. resist. (Ω.m)	44.0 (1.8)	51.0 (1.7)	55.0 (4.0)
Appar. permea. (10^{-18} m²)	100.5 (38.4)	111.3 (13.5)	119.2 (10.1)

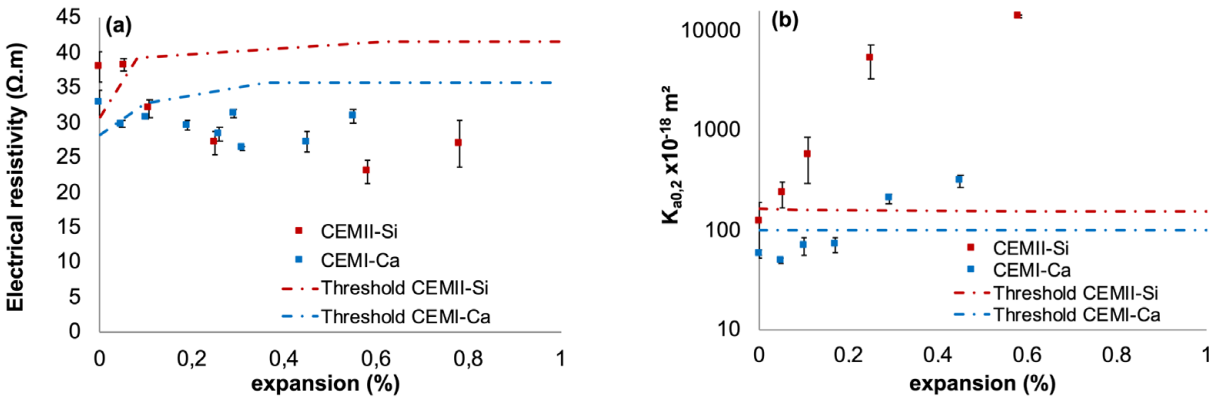

FIGURE 9. Electrical resistivity (a) and apparent gas permeability (b) versus the expansion.

3.5. Mechanical properties

The compressive strength measurements show the impact of the heat treatment on the mechanical properties. The compressive strength and static elasticity modulus values are given on time for the reference concretes (CEMII-Si and CEMI-Ca) in Table 5.

The reference concretes CEMII-Si-ref and CEMI-Ca-ref have compressive strengths of 34 MPa and 44 MPa, respectively, at 35 days. The compressive strengths of CEMII-Si and CEMI-Ca are lower, at 23 MPa and 29 MPa, respectively. These values lead to a variation of about 2 MPa (test repeatability of 8%). The reduction of the compressive strength by the heat treatment can be explained by the occurrence of damage in concrete and by the variation of hydrates (24). The compressive strength of CEMI-Ca and CEMI-Ca-ref concretes remains higher than those of other concretes and increases with time following the hydration process (Table 5). This difference is explained by the fact that these concretes contain a larger amount of cement and a lower W/C ratio, and also because the presence of limestone aggregates in the formulation improves the ITZ. The CEMII-Si and CEMI-Ca show compressive strength that remains stable during the initiation of the pathology. However, during the acceleration phase, the strength decreases spontaneously and then stabilizes at the end of the acceleration period (Figure 10a). The decrease of compressive strength is 30% and 20% for the CEMII-Si and CEMI-Ca concretes, respectively, at the half of expansion.

Depending on the chosen criterion, the detection of DEF by the measurement of compressive strength takes place between 0.11 and 0.29% of expansion, at the beginning of the acceleration phase. This range of expansion is also excessive regarding the appearance of visual defects (12, 30).

The evolutions of elastic modulus for CEMII-Si-ref and CEMI-Ca-ref reference concretes show small changes between 35 and 190 days (Table 5). The modulus is still higher for CEMII-Si-ref concrete (equal to 40 GPa) than for CEMI-Ca-ref concrete (31 GPa) at 35 days. In comparison with reference concretes, only CEMII-RSI-Si concrete shows a decrease of elastic modulus caused by the heat treatment. In this case, the lower compressive strength and the nature of aggregate used could explain this higher damage.

In Figure 10b, CEMII-Si and CEMI-Ca concretes with DEF reveal that the modulus decreases progressively during the expansion. A significant decrease in the modulus is observed for swelling of around 0.2% during the acceleration phase of the pathology. At this time, the modulus decreases by 40% and 50% for the CEMII-Ca and CEMI-Si concretes, respectively. The loss of elastic modulus seems to be proportional to the expansion rate caused by the pathology. However, the stress exerted in this test reaches one third of the compressive strength. In addition, a 3 MPa pre-loading strength is applied during the measurement. When the strong loss of compressive strength occurs (of about 0.2% of expansion), the

Table 5. Mechanical values for reference concretes on time (average values and deviation standard).

CEMII-Si-ref	35 d	91 d	180 d
Comp. strength (MPa)	34.0 (2.1)	34.1 (1.3)	38.3 (0.5)
Static modul. (GPa)	40.4 (2.4)	39.4 (0.4)	43.3 (0.9)
CEMI-Ca-ref	35 d	90 d	180 d
Comp. strength (MPa)	43.5 (1.5)	48.2 (1.4)	49.0 (0.3)
Static modul. (GPa)	31.9 (0.5)	32.1 (0.5)	33.0 (0.6)

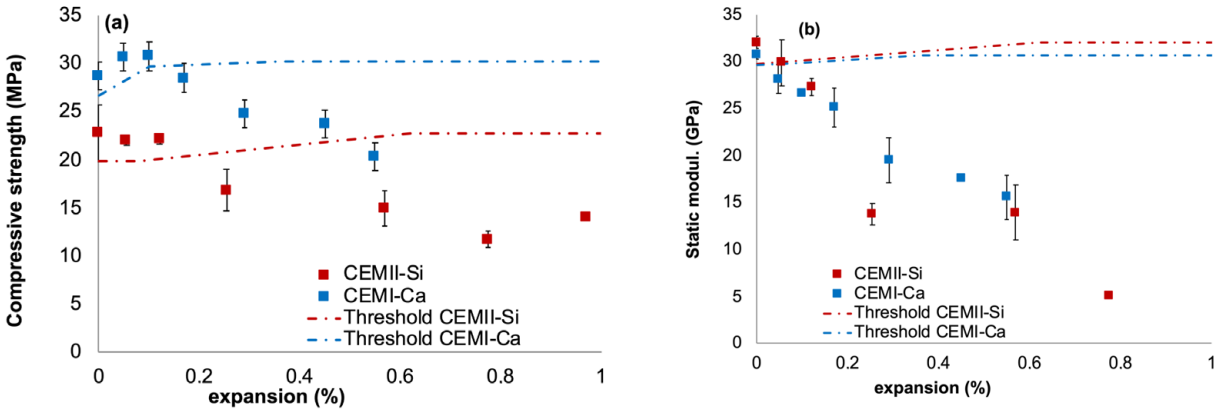

Figure 10. Compressive strength (a) and elastic modulus (b) versus the expansion.

value of the elastic modulus becomes difficult to be quantified. These results are not in agreement with those of Al Shamaa et al., who show no decrease of elastic modulus during the latent period (31).

Depending on the chosen criterion, the detection of DEF by the measurement of elastic modulus takes place between 0.05 and 0.1% of expansion, during the latent period.

4. DISCUSSION

With the used tests in this experimental program, it possible to detect DEF at the beginning of the expansion, during the latent phase. Table 6 summarizes all the expansion values at the time of detection of DEF presented in the experimental results.

Microscopic observations showed the evolution of ettringite formation during expansion in the material. Some physical measurements related to the transfer properties allowed DEF to be detected during the latent phase and measurements of the gas permeability and electrical resistivity appear to provide a good durability indicator for the detection of DEF. CEMI-Ca concrete showed a later increase in permeability than CEMII-Si. The improvement of the ITZ in the case of limestone aggregates seems to reduce the cracks generated at this interface during DEF damage (27). Moreover, a higher damage of CEMII-Si concrete caused by the thermal treatment has been observed by a loss of elastic modulus, thus, allowing the cracks in the concrete to be less percolating.

The electrical resistivity tests showed significant sensitivity (test repeatability of 10.5%), the detection being effective from the latent phase. The electrical resistivity decreased by 16% and 10% for the CEMII-Si and CEMI-Ca concretes, respectively, for expansions of 0.12% and 0.19%. Since the electrical resistivity of the reference concretes increased substantially from 35 days to 180 days (25%). The decrease in the resistivity associated with the development of the pathology seems to be significant. However, its sensitivity to water content could make electrical resistivity difficult to use for damaged structures (32).

Elastic modulus measurements also detected the presence of DEF during the latent period. A continuous decrease was observed throughout the development of the pathology. A 15% loss of modulus associated with a swelling of 0.11% was observed for each concrete. The compressive strength of the CEMII-Si and CEMI-Ca concretes damaged by DEF decreased by 26% and 14% respectively for expansions of 0.25% and 0.29%. This loss of compressive strength in the half phase of acceleration the detection of the pathology. Three durability indicators made it possible to detect DEF earlier, during the latent phase for laboratory specimens, the gas permeability, the electrical resistivity and the elastic modulus.

Figure 11a shows the evolution of the damage as a function of the expansion for the two concretes damaged by DEF. The damage was proportional to the expansion due to DEF. The damage was calculated from the elastic modulus according to Equation [2]:

$$D = 1 - \frac{E_i}{E_0} \qquad [2]$$

With: E_i elastic modulus measured during DEF development,
E_0 elastic modulus for concrete reference (without degradation).

A study (33), coupling Alkali-Silica Reaction (ASR) and DEF on concrete shows an almost linear trend. The loss of damage as a function of the expansion is in accordance with these results (33).

Figure 11b shows the evolution of air permeability (ratio between apparent value measured during DEF degradation and reference value (Table 4)) as a function of the damage presented in Figure 11a for the two concretes. The increase in permeability seems to be an exponential function of the damage. This exponential trend is harder to see for CEMII-Si concrete. However, the damage caused by the heat treatment could explain the earlier appearance of percolating path for CEMII-Si concrete. For the investigated concretes, the use of concrete composition with a lower W/C ratio and containing limestone aggregates seems to improve the durability of DEF affected concrete. The percolating paths in CEMI-Ca concrete specimens would appear at around 20% of damage, at the beginning of the acceleration phase of the pathology. For the CEMI-Si concrete, the percolating paths appear for slight damage, around 7%, causing a considerable increase of the air flow through the material.

Table 6. Summary of the evolution of the properties at detection for the CEMII-Si and CEMI-Ca concretes.

	Expansion at detection (%)		DEF phase
	CEMII-Si	CEMI-Ca	
Electrical resistivity	0.05 - 0.11	0.05 - 0.11	Latent phase
Gas permeability	0.05	0.17 - 0.29	Latent phase
Elastic modulus	0.05 - 0.11	0.05 - 0.11	Latent phase
Compressive strength	0.11 - 0.25	0.17 - 0.29	Acceleration phase

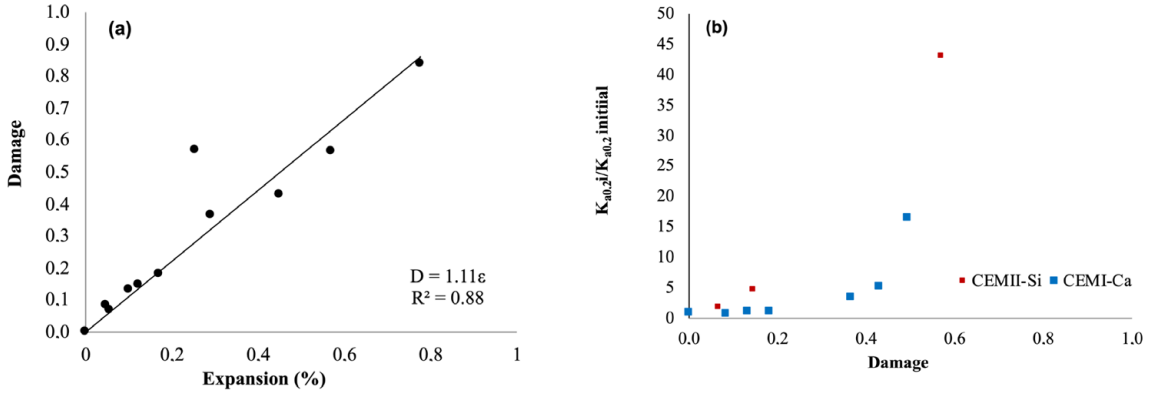

FIGURE 11. Evolution of the damage (calculated with elastic modulus) as a function of expansion (a) and of the apparent permeability rate as a function of damage (b).

5. CONCLUSIONS

An experimental investigation has been carried out to characterize DEF impact on measurable physical and mechanical properties of concrete. The second aim was to evaluate the evolution of the properties that have an impact on the tightness of concrete. Several physico-chemical and mechanical properties were measured by the use of a large quantity of samples. These tests were performed on two concretes showing a high swelling potential. Original results have been obtained:

- Electrical resistivity and gas permeability are sensitive to the expansion generated by DEF. However, the electrical resistivity could be difficult to use for damaged structures.
- For a same expansion, the apparent permeability increase is greater for concrete containing siliceous aggregate than for concrete with limestone aggregate.
- The measurement of the elastic modulus and electrical resistivity seems to allow the detection of DEF during the latent period.
- Three durability indicators seem to be relevant for the detection and the monitoring of pathology: gas permeability, electrical resistivity, and elastic modulus.
- For the investigated concretes, the loss of tightness related to the presence of DEF occurs for less than 20% of damage.

ACKNOWLEDGEMENTS

The authors thank the Institute of Radioprotection and Nuclear Safety (IRSN) for its financial support.

AUTHOR CONTRIBUTIONS:

Conceptualization: A. Pichelin; Formal analysis: A. Pichelin, M. Carcassès, F. Cassagnabère, S. Multon, G. Nahas; Funding acquisition: G. Nahas; Methodology and investigation: A. Pichelin, M. Carcassès, F. Cassagnabère, S. Multon, G. Nahas; Project administration: M. Carcassès et G. Nahas; Writing, original draft: A.Pichelin; Writing, review & editing: A. Pichelin, M. Carcassès, F. Cassagnabère, S. Multon, G. Nahas.

REFERENCES

1. Brunetaud, X. (2005) Étude de l'influence de différents paramètres et de leurs interactions sur la cinétique et l'amplitude de la réaction sulfatique interne au béton. PhD thesis, École Centrale de Paris (http://www.theses.fr/2005ECAP1025).
2. Scherer, G. (1999) Crystallization in pores. *Cem. Conc. Res.* 29, 1347-1358. https://doi.org/10.1016/S0008-8846(99)00002-2.
3. Mehta, P.K. (1973) Mechanism of expansion associated with ettringite formation. *Cem. Conc. Res*. 3, 1-6. https://doi.org/10.1016/0008-8846(73)90056-2.
4. Scrivener, K.L.; Taylor, H.F.W. (1993). Delayed ettringite formation: a microstructural and microanalytical study. *Adv. Cem. Res.* 5 [20], 139-146. https://doi.org/10.1680/adcr.1993.5.20.139.
5. Diamond, S. (1996) Delayed ettringite formation – Processes and problems. *Cem. Conc. Comp.* 18, 205-215. https://doi.org/10.1016/0958-9465(96)00017-0.
6. Li, G.; Le Bescop, P.; Moranville, M. (1995) Expansion mechanism associated with the secondary formation of the U phase in cement-based systems containing high amounts of Na SO . *Cem. Conc. Res.* 26 [2], 195-201. https://doi.org/10.1016/0008-8846(95)00199-9.
7. Zhang, Z.; Olek, J.; Diamond, S. (2002) Studies on delayed ettringite formation in heat-cured mortars II. Characteristics of cement that may be susceptible to DEF. *Cem. Conc. Res*. 17, 1737-1742. https://doi.org/10.1016/S0008-8846(02)00894-3.
8. Leklou, N. (2008) Contribution à la connaissance de la réaction sulfatique interne, PhD thesis, Université Toulouse III.
9. Fu, Y.; Ding, J.; Beaudoin, J.J. (1997) Expansion of Portland cement mortar due to internal sulfate attack. *Cem. Conc. Res*. 27, 1299-1306. https://doi.org/10.1016/S0008-8846(97)00133-6.
10. Kchakech, B. (2016) Étude de l'influence de l'échauffement subi par un béton sur le risque d'expansions associées à la réaction sulfatique interne. PhD thesis Université Paris-Est.
11. Graf, L. (2007) Effect of relative humidity on expansion and microstructure of heat-Cured mortars. RD139, Portland Cement Association, Skokie, Illinois, USA, (2007).
12. Al Shamaa, M. (2012) Étude du risque de développement d'une réaction sulfatique interne et de ses conséquences dans les bétons de structure des ouvrages nucléaires. PhD thesis, Université Paris-Est.
13. Jabbour, J. (2018) Méthodes d'essais de vieillissement accéléré des bétons à l'échelle des ouvrages. PhD thesis, Université Paris-Saclay.
14. NF EN 197-1 (2012). Ciment – Partie 1: Composition, spécifications et critères de conformité des ciments courants, AFNOR, (2012).

15. ODOBA project (2018) by IRSN https://www.irsn.fr/EN/Research/Research-organisation/Research-programmes/Odoba-project/Pages/ODOBA.aspx.
16. NF P18-404 (1981) Bétons - Essais d›étude, de convenance et de contrôle - Confection et conservation des éprouvettes, AFNOR (1981).
17. NF P18-400 (1981) Bétons - Moules pour éprouvettes cylindriques et prismatiques, AFNOR (1981).
18. Méthode d'essai n°66 (2007). Réactivité d'un béton vis-à-vis d'une réaction sulfatique interne. Laboratoire Central des Ponts et Chaussées (2007).
19. Leklou, N.; Aubert, J-E. ; Escadeillas, G. (2013) Influence of various parameters on heat-induced internal sulphate attack. *Europ. J. Env. Civ. Eng.* 17, 141-153. https://doi.org/10.1080/19648189.2012.755338.
20. PerfDuB (2017) Determination of the resistivity of saturated concrete. IREX (2017).
21. XP P18-463, 2011. Bétons - Essai de perméabilité aux gaz sur béton durci, AFNOR (2011).
22. NF EN 12390-3 (2003) Essais pour béton durci - Partie 3: Résistance à la compression des éprouvettes, AFNOR, (2003).
23. NF EN 12390-13 (2014) Essai pour béton durci - Partie 13: détermination du module sécant d'élasticité en compression, AFNOR (2014).
24. Al Shamaa, M.; Lavaud, S.; Divet, L.; Colliat, J-B.; Nahas, G.; Torrenti, J.-M. (2016) Influence of limestone filler and of the size of the aggregates on DEF. *Cem. Conc. Comp*. 71, 175-180. https://doi.org/10.1016/j.cemconcomp.2016.05.007.
25. Grattan-Bellew, P.E.; Beaudoin, J.J.; Vallée, V-G. (1998) Effect of aggregate particle size and composition on expansion of mortar bars due to delayed ettringite formation. *Cem. Conc. Res.* 28 [8], 1147-1156. https://doi.org/10.1016/S0008-8846(98)00084-2.
26. Bentz, D.P.; Ardani, A.; Barrett, T.; Jones, S.Z.; Lootens, D.; Peltz, M.A.; Sato, T.; Stutzman, P.E.; Tanesi, J.; Weiss, W.J. (2015) Multi-scale investigation of the performance of limestone in concrete. *Cons. Build. Mat.* 75, 1-10. https://doi.org/10.1016/j.conbuildmat.2014.10.042.
27. Yang, R.; Lawrence, C.D.; Sharp, J.H. (1999) Effect of type of aggregate on delayed ettringite formation. *Adv. Cem. Res.* 11 [3], 119-132. https://doi.org/10.1680/adcr.1999.11.3.119.
28. Bouzabata, H.; Multon, S.; Sellier, A.; Houari, H. (2012) Effects of restraint on expansion due to delayed ettringite formation. *Cem. Concr. Res.* 42, 1024–1031. https://doi.org/10.1016/j.cemconres.2012.04.001.
29. Al Shamaa, M.; Lavaud, S.; Divet, L.; Nahas, G.; Torrenti, J.M. (2015) Influence of relative humidity on delayed ettringite formation. *Cem. Concr. Comp.* 58, 14-22. https://doi.org/10.1016/j.cemconcomp.2014.12.013.
30. Bruneteaud, X.; Divet, L.; Damidot, D. (2008) Impact of unrestrained Delayed Ettringite Formation-induced expansion on concrete mechanical properties. *Cem. Conc. Res.* 38, 1343-1348. https://doi.org/10.1016/j.cemconres.2008.05.005.
31. Al Shamaa, M.; Lavaud, S.; Divet, L.; Nahas, G.: Torrenti, J.M. (2014) Coupling between mechanical and transfer properties and expansion due to DEF in a concrete of a nuclear power plant. *Nucl. Eng. Desig.* 266, 70-77. https://doi.org/10.1016/j.nucengdes.2013.10.014.
32. Rivard, P.; Saint-Pierre, F. (2009) Assessing alkali-silica reaction damage to concrete with non-destructive methods: From the lab to the field. *Cons. Buil. Mat.* 23, 902–909. https://doi.org/10.1016/j.conbuildmat.2008.04.013.
33. Martin, R-P.; Sanchez, L.; Fournier, B.; Toutlemonde, F. (2017) Evaluation of different techniques for the diagnosis & prognosis of Internal Swelling Reaction (ISR) mechanisms in concrete. *Construct. Build. Mater.* 156, 956–964. https://doi.org/10.1016/j.conbuildmat.2017.09.047.